The thermal effect of 2.45 GHz microwave radiation on rat testes

Viera Almášiová[1], Katarína Holovská[1], Veronika Šimaiová[1], Katarína Beňová[2], Adam Raček[2], Enikö Račeková[3], Marcela Martončíková[3], Jozef Mihálik[4], Františka Horváthová[4], Lucia Tarabová[5], Tomáš Slanina[6], Viera Cigánková[1]

[1]University of Veterinary Medicine and Pharmacy in Košice, Department of Anatomy, Histology and Physiology, Košice,-Slovak Republic
[2]University of Veterinary Medicine and Pharmacy in Košice, Department of Biology and Genetics, Košice, Slovak Republic
[3]Slovak Academy of Sciences, Institute of Neurobiology, Košice, Slovak Republic
[4] Šafárik University, Medical Faculty, Department of Anatomy, Košice, Slovak Republic
[5]University of Veterinary Medicine and Pharmacy, Department of Pathological Anatomy and Pathological Physiology, Košice, Slovak Republic
[6]Slovak University of Agriculture, Department of Animal Physiology, Nitra, Slovak Republic

Received June 9, 2017
Accepted December 19, 2017

Abstract

The study focused on the effect of microwave radiation at a dose which commonly does not lead to tissue heating, however, in the rat testes it resulted in accumulation of heat. Adult rats were exposed to whole body pulse radiation at a frequency of 2.45 GHz and mean power density of 28 W/m^2, for 3 h a day for the duration of 3 weeks. Immediately after each irradiation, the body temperature and the testicular temperature were measured in the control and experimental animals. Samples for histological and immunohistochemical analysis were taken after the last irradiation and processed for light and transmission electron microscopy. An evaluation of spermatozoa motility was performed using computer-assisted sperm analysis. Although the body temperature of the rats was not elevated after the irradiations, the testicular temperature was significantly increased ($P < 0.004$). Testes of the experimental animals had considerably dilated and congested blood vessels and the seminiferous epithelium showed degenerative changes. The Leydig cells showed no obvious structural abnormalities. Transmission electron microscopy revealed ultrastructural changes in developing sex cells, Sertoli cells, and endothelial cells. An intensified immunoreactivity to superoxide dismutase 1 was found in spermatogonia and Leydig cells in the experimental animals. Results of the present study revealed a distinctly adverse effect of microwave radiation on the thermoregulatory capability and histological structure of rat testes as well as an oxidative damage of the tissue. The scientific knowledge confirming or denying the thermal effect of microwave radiation on living tissue is scarce and thus the present study may be regarded as unique and helpful to clarify the issue.

Non-ionizing radiation, male gonads, structure, ultrastructure, immunohistochemical analysis

Fertility problems affect the human population worldwide. A number of reports have found an association between exposure to radiofrequency electromagnetic radiation generated by wireless devices such mobile phones, cordless phones, microwave ovens, radars, Wi-Fi and base stations and the negative effect on different reproductive indices (Panagopoulos 2013). These studies have attributed most of the male reproductive system injury to the non-thermal radiation effect but have not excluded its potential thermal effect. Thus, the occurrence of a thermal effect of microwave electromagnetic radiation (MW EMR) within tissues still remains to be further clarified. Tissues are rich in water molecules which are polar and susceptible to the effect of MW EMR. Their vibrations result in a gain of energy in the form of heat which causes an elevation in the temperature of the tissue. The body is made up of a mixture of types of tissues which may result in a non-uniform distribution

Address for correspondence:
Doc. MVDr. Viera Almášiová, PhD
Department of Anatomy, Histology and Physiology
University of Veterinary Medicine and Pharmacy
Komenského 73, 04181 Košice, Slovak Republic

Phone: +421 918 967942
E-mail: viera.almasiova@uvlf.sk
http://actavet.vfu.cz/

of heat and occurrence of the so-called hot spots. Relevant safety standards (ICNIRP 1998, IEEE 2003) determined safe power density limits for a specific frequency based on the average whole body specific absorption rate – SAR (0.4 $w \cdot kg^{-1}$ occupational exposure, and 0.08 $w \cdot kg^{-1}$ general public exposure), but in some areas considerably higher temperatures may occur than in others, and this should be elucidated. From this point of view, organs which are considered more sensitive to the thermal effect are the eyes and the testes. There is a technical problem of establishing the quantity of heat and its spatial distribution in the body due to difficulties with direct measurements.

The present study was designed to determine the potential thermal and/or non-thermal effects of immediate, whole body electromagnetic irradiation of rat testes, using sexually mature Wistar rats irradiated by pulsed electromagnetic field at a frequency of 2.45 GHz and mean power density of 28 W/m^2, for 3 h a day for 3 weeks.

Materials and Methods

Experimental design

The experiment was carried out on sexually mature male rats of the Wistar strain (n = 20) which were randomly assigned to control (n = 10) and experimental (n = 10) groups. The rats were kept in cages (two rats in each), at controlled temperature of 21 ± 1 °C, and had *ad libitum* access to water and food (Larsen diet). The light was turned off or on using a 12 h regimen. The experimental rats were irradiated in a purpose-designed chamber by a pulse MW EMR at frequency of 2.45 GHz and mean power density of 28 W/m^2, for 3 h a day for the duration of 3 weeks. Uniformity of the electromagnetic field was checked with a spectral analyser. The experiment was conducted at the Institute of Neurobiology, Slovak Academy of Sciences. The care and use of animals were approved by the Ethics Committee of the Institute of Neurobiology (Ro 2792/15-221/2), Slovak Academy of Sciences, and the State Veterinary and Food Administration of the Slovak Republic.

Measurement of total body temperature and local scrotal temperature

Immediately before and after each irradiation, the body and local temperature was measured both in the control and the experimental animals. The body temperature was measured in the rectum by a Digital Veterinary thermometer Adtemp ™ 422 (China). The local testicular temperature in the scrotal region was determined by the thermocamera FLIR E40 (FLIR Systems OU, Estonia). The thermographs were evaluated by the software FLIR Tools, version 2.0 (FLIR systems, Ins., Wilsonville, USA). Statistical analysis was performed by paired *t*-test (GraphPad Prism, GraphPad Prism®). The results are expressed as mean ± SEM.

Histopathological analysis – light and transmission electron microscopy (LM, TEM)

The animals were anaesthetized by *i. p.* injection of xylazine and ketamine, sacrificed by decapitation and their testes were sampled for histopathological examination. The whole right testis was obtained from each animal and processed for light microscopy. The samples were fixed in mDF solution (Latendresse et al. 2002) for 24 h, dehydrated and finally embedded in paraffin. Five µm thick tissue sections were stained with haematoxylin and eosin (HE), examined under the light microscope Zeiss Axio Lab A1 (Zeiss, Germany) and documented with a camera Axio Cam ERc 5 (Zeiss, Germany). For transmission electron microscopy examination, four tissue samples up to 1 mm^3 were obtained from different parts (more superficial and deeper) of the left sided testis of each control and experimental animal and fixed by immersion in 3% glutaraldehyde and postfixed in 1% osmium tetraoxide (both in 0.1 M phosphate buffer, pH 7.3). After dehydration in acetone, they were transferred to propylene oxide and embedded in Durcupan™ ACM (Sigma-Aldrich Chemie GmbH, Germany). Sections of the specimen were cut using the ultramicrotome LKB Nova (Sweden). Semi-thin sections were stained with toluidine blue and examined under the light microscope Zeiss Axio Lab A1. Ultrathin sections were double contrasted with uranyl-acetate and lead citrate and examined under the electron microscope Tesla BS 500 (Czech Republic).

Superoxide dismutase 1 (SOD1) analysis

Ten sections (5 µm thick) from each paraffin block were placed on histological slides, deparaffined and washed with phosphate buffer (PBS-Tween 20). Endogenous peroxidase activity was blocked by bathing the sections in 3% H_2O_2 solution of methanol. Then the sections were washed with PBS-Tween 20, citrate buffer and PBS-Tween 20 again. The blockage of nonspecific background reaction was provided by 5% milk buffer and primary monoclonal antibodies (#ADI-SOD-100-D, Enzo Life Science, USA) were applied. The sections were then washed with PBS-Tween 20 and the secondary biotinylated antibody (#K0690, Dako, Glostrup, Denmark) was added. Then they were washed again with phosphate buffer and streptavidin peroxidase was applied. After the washing, the proteins were visualized by 3, 3-diaminobenzidin (DAB, #SK4100, Vector Laboratories, USA) solution. The sections were then washed in distilled water and counterstained with haematoxylin.

Computer-assisted sperm analysis (CASA)

Rat spermatozoa were obtained by puncturing the distal cauda epididymidis and subsequently dispersed up to 1/100 in saline. Measurements were performed at three intervals - immediately after collection (time 0), 1 h after collection (time 1) and 2 h after-collection (time 2). Samples were kept in a thermostat at 37 °C. Spermatozoa motility was measured by CASA and evaluated by the SpermVision™ (Minitube, Tiefenbach, Germany) software connected to the Olympus BX 51 (Olympus, Japan) microscope. Each sample was placed in a 10 μm deep-scale compartment of the Makler Counting Chamber (Sefi-Medical Instruments, Germany), and within each measurement, the CASA system evaluated mobility indices from at least 7 compartments. The results were statistically processed by SAS (Scheffe test). The following indicators were monitored in each sample:

MOT - motility (% of moving sperm, speed above 5 μm/s)
PRO - progressive motility (% of progressive moving sperm, velocity above 20 μm/s)
DAP - distance average path (μm)
DCL - distance curved line (μm)
DSL - distance straight line (μm)
VAP - velocity average path (μm/s)
VCL - curved line velocity (μm/s)
VSL - straight line velocity (μm/s)
STR - straightness of movement
LIN - linearity [VSL: VCL]
WOB - wobble [VAP: VCL]
ALH - amplitude of lateral head displacement (μm/s)
BCF - beat cross frequency (Hz)

Results

Total body temperature and thermographic examination

The body temperature of experimental and control animals did not differ either before or after the irradiation (the average temperature was 36.9 ± 0.8 °C), whereas the local temperature of the testes in the experimental rats evaluated by the thermocamera increased significantly ($P < 0.004$) after each irradiation. The average testicular temperature in the experimental rats was 29.45 ± 0.07 °C before irradiation and 30.25 ± 0.10 °C after irradiation. Thus, the testicular temperature increased by 0.8 ± 0.03 °C (Plate IV, Fig. 1).

Histopathological observation and immunohistochemical analysis

The testes of the experimental rats had markedly congested and dilated blood vessels within both the tunica albuginea (Plate IV, Fig. 2a) and the interstitium (Plate IV, Fig. 2b). The seminiferous epithelium contained empty spaces between the developing spermatogenic cells, and immature germ cells were often congregated within the lumen of the tubules. The Leydig cells appeared relatively intact (Plate IV, Fig. 2b). Transmission electron microscopy revealed degenerative changes of developing spermatogenic cells as well as somatic Sertoli cells. The size of Sertoli cells was often reduced and their cytoplasm contained many vacuoles and swollen mitochondria. In some sporadic cases, the Sertoli cells revealed clear signs of necrotization, such as the strongly electron-dense cytoplasm with evidently broken organelles and numerous vacuoles. The individual forms of developing sex cells had damaged organelles and possesed many small round electronlucent vacuoles. Numerous small and irregular empty spaces between the cells of seminiferous epithelium as well as affected tight junctions between the adjacent Sertoli cells were also clearly seen (Plate IV, Fig. 3a). The interstitial space contained unaffected Leydig cells and fibrocytes, but the blood capillaries revealed broken intercellular connections between the adjacent endothelial cells and basement membrane of uneven thickness (Plate IV, Fig. 3b). While the most extensive immunoreaction to SOD1 was found in the residual bodies within the seminiferous tubules of the control rats (Plate V, Fig. 4a), the highest immunoreactivity to SOD1 was seen in spermatogonia and Leydig cells in the seminiferous tubules of experimental animals (Plate V, Fig. 4b).

Computer-assisted sperm analysis (CASA)

The indicators of spermatozoa motility such the MOT, DAP, DCL, VAP, VCL, PRO, DSL, VSL, STR, LIN, ALH and BCF were significantly ($P < 0.01$) affected in the irradiated rats. The most significant changes were observed 1 h after taking of sample collection (time 1). These data show that the MW EMR adversely affected almost all of the monitored indicators of spermatozoa motility (Table 1).

Discussion

The deleterious effect of microwave radiation on the reproductive functions has been the subject of frequent discussions because modern devices such as mobile phones or laptop computers are often held in close proximity of the reproductive organs (Al Damegh 2012; Kesari et al. 2013; Naziroglu et al. 2013). The testes of most mammals including humans are superficially located and require slightly lower temperature for their optimal function. Because of their specific position they may absorb relatively high amount of energy during the whole body irradiation. Due to their specific anatomical arrangement, the thick dense connective tissue envelope tunica albuginea, which restricts surface conduction for temperature control, is an important target for the biological effect of microwave radiation (Kesari et al. 2013).

In the present study, the effects of pulse microwave EMR on the body and testicular temperature was investigated by a thermometer and a thermocamera. The results showed that the whole body microwave irradiation had an adverse effect on the testicular temperature. The local testicular temperature in irradiated animals increased by 0.8 ± 0.08 °C which corresponded to our histopathologic observations. The blood vessels within the tunica albuginea and interstitium were clearly congested and dilated which indicated an intensified effort of the organ to dissipate the heat. The scientific knowledge confirming this phenomenon is scarce and thus the present study may be regarded as unique. The increased local testicular temperature caused diffuse degenerative changes in the seminiferous epithelium such the formation of small empty spaces between the cells of the seminiferous epithelium and sloughing of immature germ cells. Examination by electron microscopy showed diffuse degenerative changes, such as vacuolisation of cytoplasm and damaged organelles in germ cells and Sertoli cells, detachment of the adjacent Sertoli cells and interrupted intercellular junctions between the adjacent endothelial cells in blood capillaries. Histopathological changes observed in the present study are consistent with other relevant studies, where the authors also recorded cellular vacuolisation, reduction in the number of germ cells and cellular disorganization (Ribeiro et al. 2007; Usikalu et al. 2010), severing of the spermatogenic cells (El-Bediwi et al. 2011), degeneration and necrotization of the cells of the germinal epithelium, and a decrease in Sertoli cells (Khayyat 2011). At the level of electron microscopy, major mitochondrial damage has been also found (Tenorio et al. 2012).

Many authors consider oxidative stress as one of the most frequently recorded phenomenon associated with microwave-induced tissue injury. Liu et al. (2013) determined in a modified comet assay that radiofrequency EMR has insufficient energy for the direct induction of DNA strand breaks, however, it produces genotoxicity through oxidative DNA damage in the male germ cells. These findings are further supported by Al Damegh (2012), Meena et al. (2013), Naziroglu et al. (2013) and Jelodar et al. (2014), who evaluated various stress-related indices (e.g. catalase and lactate dehydrogenase isoenzyme activity, glutathione and glutathione peroxidase levels, ROS - reactive oxygen species, and others) in testicular tissue and concluded that MW radiation induced oxidative stress with subsequent DNA damage of testicular cells. The MW EMR also promotes apoptosis through the ROS formation (Hou et al. 2014). These results are in agreement with our

Table 1. Semen indicators of control and experimental animals evaluated by the computer-assisted sperm analysis (CASA).

Time (h)	Indicator	Control animals	Experimental animals
		x ± SE	
0	MOT	54.26 ± 1.65	47.54 ± 2.26
1		47.45 ± 1.96	6.79 ± 1.87**
2		12.14 ± 1.16	14.18 ± 1.71
0	PRO	27.40 ± 1.32	23.62 ± 1.66
1		20.51 ± 1.22	10.98 ± 1.04*
2		3.43 ± 0.51	3.78 ± 0.87
0	DAP	24.58 ± 0.81	27.53 ± 0.77
1		24.40 ± 0.93	25.88 ± 1.70**
2		17.96 ± 2.61	12.59 ± 2.22
0	DCL	37.59 ± 1.06	42.26 ± 0.94
1		36.26 ± 1.29	37.38 ± 2.27**
2		26.22 ± 3.72	17.59 ± 2.90
0	DSL	18.77 ± 0.74	19.65 ± 0.59
1		17.87 ± 0.54	17.99 ± 1.10*
2		12.17 ± 1.74	8.10 ± 1.17
0	VAP	61.95 ± 2.24	67.20 ± 1.91
1		59.19 ± 2.54	64.50 ± 4.37**
2		44.74 ± 6.74	29.58 ± 4.85
0	VCL	94.16 ± 2.98	102.50 ± 2.44
1		87.78 ± 3.57	92.69 ± 5.92**
2		66.09 ± 9.62	41.38 ± 6.44
0	VSL	47.61 ± 2.04	48.31 ± 1.60
1		43.62 ± 1.63	44.49 ± 2.68*
2		30.93 ± 4.60	19.70 ± 2.84*
0	STR	0.76 ± 0.01	0.72 ± 0.01
1		0.74 ± 0.01	0.68 ± 0.03
2		0.57 ± 0.06	0.43 ± 0.06*
0	LIN	0.50 ± 0.01	0.47 ± 0.01
1		0.50 ± 0.01	0.47 ± 0.02
2		0.42 ± 0.05	0.31 ± 0.05*
0	WOB	0.65 ± 0.01	0.65 ± 0.01
1		6.67 ± 0.01	0.66 ± 0.02
2		0.56 ± 0.06	0.43 ± 0.06
0	ALH	5.92 ± 0.17	6.34 ± 0.21*
1		5.37 ± 0.14	4.74 ± 0.21
2		3.64 ± 0.42	2.61 ± 0.38*
0	BCF	18.95 ± 0.68	19.74 ± 0.59
1		18.77 ± 0.48	18.50 ± 1.01
2		16.51 ± 2.37	9.90 ± 1.56*

Note: Values are calculated as 0 (immediately after sampling), 1 (1 hour after sampling) and 2 (2 hours after sampling). MOT - motility, PRO - progressive motility, DAP - distance average path, DCL - distance curved line, DSL - distance straight line, VAP - velocity average path, VCL - curved line velocity, VSL - straight line speed, STR - straightness of movement, LIN - linearity, WOB - wobble, ALH - amplitude of lateral head displacement, BCF - beat cross frequency, x - mean, SE - standard error. There were significant differences at $*P < 0.05$, $**P < 0.01$ between control and experimental animals (x ± SE).

observation of an enhanced SOD1 immunoreactivity in spermatogonia and Leydig cells in the testes and presence of sporadic necrotizing cells of the seminiferous epithelium of irradiated animals. Next important biological effects of MW radiation including reproductive outcomes are described in more detail in the review of Kesari et al. (2013).

Many studies show that MW radiation has an adverse effect on the male reproductive capacity through reducing semen quality. Roychoudhury et al. (2009) and Lukac et al. (2011) evaluated spermatozoa motility by the CASA method and noted its clear inhibition in irradiated animals. The analyses of the use of different wireless equipments on human semen also proved their negative effect - the number of spermatozoa of abnormal morphology increased (Wdowiak et al. 2007) and the percentage of sperm cells in vital progressing motility in the semen decreased (Baste et al. 2008; Liu et al. 2014). In addition to the decrease in spermatozoa viability and motility, a reduction of the total antioxidant capacity was also found (Ghambari et al. 2013). The evaluation of spermatozoa motility by CASA in the present work is consistent with the above mentioned findings.

In conclusion, the whole body, pulse radiation at a frequency of 2.45 GHz and mean power density of 28 W/m^2, for 3 h a day for the duration of 3 weeks had an adverse effect on rat testicular tissue morphology and spermatozoa motility. The results of the present study fully support the theory that microwave radiation can strongly influence the testes by the thermal effect, even though the presence of a non-thermal effect was not excluded.

Acknowledgements

This study was supported by the project of the Ministry of Education, Science, Research, and Sport of the Slovak Republic, VEGA No. 1/0214/15.

Declaration of interest

The authors report no conflict of interest.

References

Al Damegh MA 2012: Rat testicular impairment induced by electromagnetic radiation from a conventional cellular telephone and the protective effects of the antioxidants vitamins C and E. Clinics **67**: 785-792

Baste V, Riise T, Moen BE 2008: Radiofrequency electromagnetic fields, male infertility and sex ratio offspring. Eur J Epidemiol **23**: 369-377

El-Bediwi AB, El-Kott AF, Saad M, Eid E 2011: Effects of electromagnetic radiation produced by mobile phone on some visceral organs of rat. J Med Sci **11**: 256-260

Ghambari M, Mortazavi SB, Khavanin A, Khazaei M 2013: The effects of cell phone waves (900 MHz-GSM Band) on sperm parameter and total antioxidant capacity in rats. Int J Fertil Steril **7**: 21-28

Hou Q, Wang M, Wu S, Ma X, An G, Lin H, Xie F 2014: Oxidative changes and apoptosis induced by 1800 MHz electromagnetic radiation in NIH/3T3 cells. Electrom Biol Med **34**: 85-92

ICNIRP 1998: Guidelines for limiting exposure to time-varying electri, magnetic and electromagnetic fields (up to 300 GHz). Health Phys **74**: 494-522

IEEE 2003: Safety standards for human exposure to radio frequency radiation and their biological rationale. Microw Magaz **4**: 22-26

Jelodar G, Nazifi S, Akbari A 2014: The prophylactic effect of vitamin C on induced oxidative stress in rat testis following exposure to 900 MHz radiofrequency wave generated by a BTS antenna model. Zahedan J Res Med Sci **16**: 19-23

Kesari KK, Kumar S, Nirala J, Siddiqui MH, Behari J 2013: Biophysical evaluation of radiofrequency electromagnetic field effects on male reproductive pattern. Cell Bioch Biophys **65**: 85-96

Khayyat LI 2011: The histopathological effects of an electromagnetic field on the kidney and testis of mice. EurAsian J Biol Sci **5**: 103-109

Latendresse JR, Warbrittion AR, Jonassen H, Creasy DM 2002: Fixation of testes and eyes using a modified Davidson's fluid: Comparison with Bouin's fluid and conventional Davidson's fluid. Toxicol Pathol **33**: 524-533

Liu C, Duan W, Xu S, Chen C, He M, Zhang L, Yu Z, Zhou Z 2013: Exposure to 1800 MHz radiofrequency electromagnetic radiation induces oxidative DNA base damage in a mouse spermatocyte-derived cell line. Toxicol Lett **218**: 2-9

Liu K, Li Y, Zhang G, Liu J, Cao J, Ao L, Zhang S 2014: Association between mobile phone use and semen quality: a systemic review and metaanalysis. Androl **2**: 491-501

Lukac N, Massanyi P, Roychoudhury S, Capcarova M, Tvrda E, Knazicka Z, Kolesarova A, Danko J 2011: *In vitro* effects of radiofrequency electromagnetic waves on bovine spermatozoa motility. J Environ Sci Health A **46**: 1417-1423

Meena R, Kumari K, Kumar J, Rajamani P, Verma HN, Kesari KK 2013: Therapeutic approaches of melatonin in microwave radiation-induced oxidative stress-mediated toxicity on male fertility patterns of Wistar rats. Electromagn Biol Med **33**: 81-91

Naziroglu M, Yüksel M, Köse SA, Özaka MO 2013: Recent reports of Wi-Fi and mobile phone – induced radiation on oxidative stress and reproductive signaling pathways in females and males. J Membrane Biol. **246**: 869-875

Panagopoulos DJ 2013: Electromagnetic interaction between environmental fields and living systems determines health and well-being. In: Kwang MH and Yoon SO: Electromagnetic fields: Principles of Biophysical Effects. Nova Science Publishers, Inc, pp 87-130

Ribeiro EP, Rhoden EL, Horn MM, Rhoden C, Lima LP, Toniolo L 2007: Effects of subchronic exposure to radio frequency from a conventional cellular telephone on testicular function in adult rats. J Urol **177**: 395-399

Roychoudhury S, Jedlicka J, Parkanyi V, Rafay J, Ondruska L, Massanyi P, Bulla J 2009: Influence of a 50 hz extra low frequency electromagnetic field on spermatozoa motility and fertilization rates in rabbits. J Environ Sci Health A **10**: 1041-1047

Tenorio BM, Jimenez GCh, de Morais RN, Peixoto ChA, de Albuquerque NR, da Silva JVA 2012: Evaluation of testicular degeneration induced by low-frequency electromagnetic fields. J Appl Toxicol **32**: 210-218

Usikalu MR, Aweda MA, Babatunde EB, Awobajo FO 2010: Low level microwave exposure decreases the number of germ cells and affect vital organs of Spraque Dawley rats. Am J Sci Indust Res **1**: 410-420

Wdowiak A, Wdowiak L, Wiktor H 2007: Evaluation of the effect of using mobile phones on male fertility. Ann Agric Environ Med **14**: 169-172

Xu S, Zhou Z, Zhang L, Yu Z, Zhang W, Wang Y et al. 2010: Exposure to 1800 MHz radiofrequency radiation induces oxidative damage to mitochondrial DNA in primary cultured neurons. Brain Res **1311**: 189-196

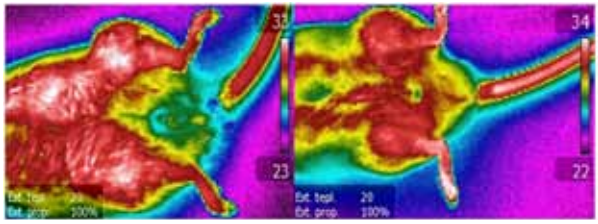

Fig. 1. Thermal images of the experimental rat showing ventral aspects of the body before (left) and after (right) the irradiation.
Note: the testicular temperature increased significantly after each irradiation by 0.8 ± 0.03 ºC ($P < 0.004$).

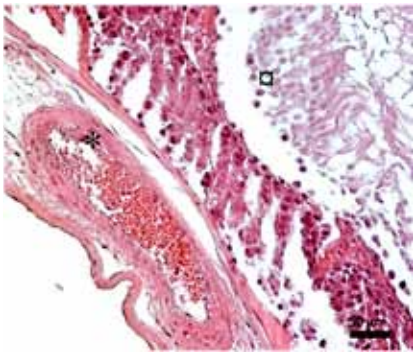

Fig. 2a. Microphotograph of the testicular tissue in experimental rat after the last irradiation. Congested and dilated blood vessel within tunica albuginea (*), desquamed immature germ cells (¤), HE, magnification × 200

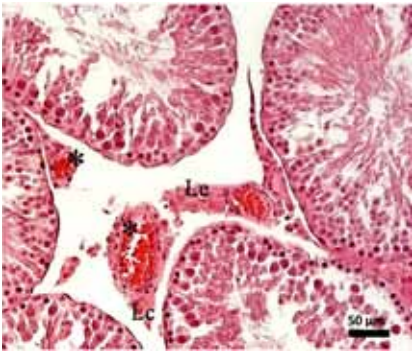

Fig. 2b. Microphotograph of the testicular tissue in experimental rat after the last irradiation. Congested and dilated blood vessels within the interstitium (*), and groups of Leydig cells with normal structure (Lc), HE, magnification × 200

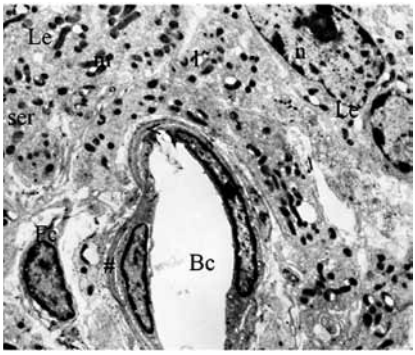

Fig. 3a. Electron micrograph of the basal compartment of seminiferous epithelium in an experimental rat after the last irradiation. Se - necrotizing Sertoli cell with damaged mitochondria (m) and numerous vacuoles (v) within electron-dense cytoplasm. Sg - spermatogonium and Sc - spermatocyte, both poor in organelles and vacuolized cytoplasm (v), » - interruptions between adjacent cells, and defective blood-testis barrier (↓), magnification × 8200

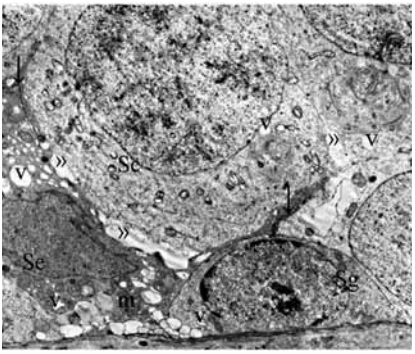

Fig. 3b. Electron micrograph of the interstitial space in an experimental rat after the last irradiation. Le – Leydig cells with characteristic nuclei (n), mitochondria (m), lipid droplets (l) and smooth endoplasmic reticulum (ser). Fc – fibrocyte with preserved ultrastructure. Bc - blood capillary with affected junction between adjacent endothelial cells (<) and unevenly thick basement membrane (#), magnification × 8800

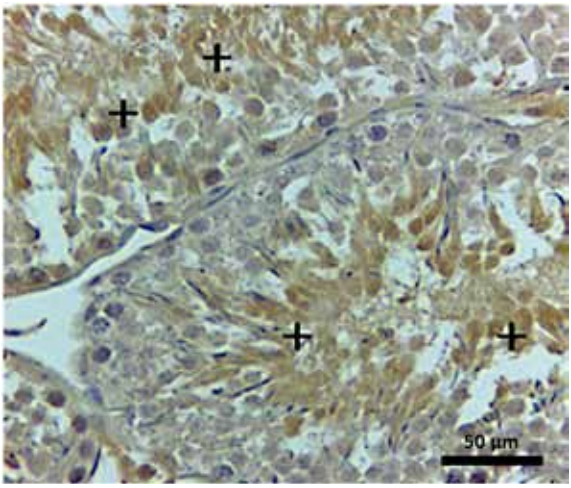

Fig. 4a. Superoxide dismutase 1 (SOD 1) analysis of testicular tissue in control rats. Immunodetection of superoxide dismutase 1 in brown - +, magnification × 400

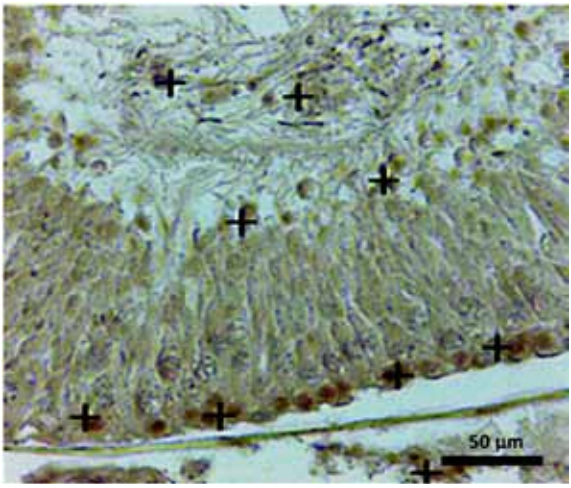

Fig. 4b. Superoxide dismutase 1 (SOD 1) analysis of testicular tissue in experimental rats after the last irradiation. Immunodetection of superoxide dismutase 1 in brown - +, magnification × 400